



Dissipation range turbulent cascades in plasmas

P. W. Terry, A. F. Almagri, G. Fiksel, C. B. Forest, D. R. Hatch et al.

Citation: [Phys. Plasmas 19, 055906 \(2012\)](#); doi: 10.1063/1.3698309

View online: <http://dx.doi.org/10.1063/1.3698309>

View Table of Contents: <http://pop.aip.org/resource/1/PHPAEN/v19/i5>

Published by the American Institute of Physics.

Related Articles

Gyrokinetic prediction of microtearing turbulence in standard tokamaks
[Phys. Plasmas 19, 055907 \(2012\)](#)

Simulation of microtearing turbulence in national spherical torus experiment
[Phys. Plasmas 19, 056119 \(2012\)](#)

Beams, brightness, and background: Using active spectroscopy techniques for precision measurements in fusion plasma research
[Phys. Plasmas 19, 056118 \(2012\)](#)

Gyrokinetic turbulent transport simulation of a high ion temperature plasma in large helical device experiment
[Phys. Plasmas 19, 042504 \(2012\)](#)

Second harmonic electromagnetic emission of a turbulent magnetized plasma driven by a powerful electron beam
[Phys. Plasmas 19, 044501 \(2012\)](#)

Additional information on Phys. Plasmas

Journal Homepage: <http://pop.aip.org/>

Journal Information: http://pop.aip.org/about/about_the_journal

Top downloads: http://pop.aip.org/features/most_downloaded

Information for Authors: <http://pop.aip.org/authors>

ADVERTISEMENT

The banner for AIP Advances. At the top, the "AIP Advances" logo is displayed, featuring the word "AIP" in blue and "Advances" in green, with several orange dots of varying sizes to the right. Below the logo, a green horizontal bar contains the text "Special Topic Section: PHYSICS OF CANCER" in white. Underneath this, the question "Why cancer? Why physics?" is written in white. To the right of the question is a blue button with the text "View Articles Now". The background of the banner is a green and yellow abstract pattern.

Dissipation range turbulent cascades in plasmas^{a)}

P. W. Terry,^{1,b)} A. F. Almagri,¹ G. Fiksel,² C. B. Forest,¹ D. R. Hatch,³ F. Jenko,³ M. D. Nornberg,¹ S. C. Prager,⁴ K. Rahbarnia,¹ Y. Ren,⁴ and J. S. Sarff¹

¹Center for Magnetic Self Organization in Laboratory and Astrophysical Plasmas, Department of Physics, University of Wisconsin-Madison, Madison, Wisconsin 53706, USA

²Laboratory for Laser Energetics, University of Rochester, Rochester, New York 13623, USA

³Max-Planck-Institut für Plasmaphysik, Garching, Germany

⁴Princeton Plasma Physics Laboratory, Princeton, New Jersey 08543, USA

(Received 7 December 2011; accepted 12 March 2012; published online 2 April 2012)

Dissipation range cascades in plasma turbulence are described and spectra are formulated from the scaled attenuation in wavenumber space of the spectral energy transfer rate. This yields spectra characterized by the product of a power law and exponential fall-off, applicable to all scales. Spectral indices of the power law and exponential fall-off depend on the scaling of the dissipation, the strength of the nonlinearity, and nonlocal effects when dissipation rates of multiple fluctuation fields are different. The theory is used to derive spectra for MHD turbulence with magnetic Prandtl number greater than unity, extending previous work. The theory is also applied to generic plasma turbulence by considering the spectrum from damping with arbitrary wavenumber scaling. The latter is relevant to ion temperature gradient turbulence modeled by gyrokinetics. The spectrum in this case has an exponential component that becomes weaker at small scale, giving a power law asymptotically. Results from the theory are compared to three very different types of turbulence. These include the magnetic plasma turbulence of the Madison Symmetric Torus, the MHD turbulence of liquid metal in the Madison Dynamo Experiment, and gyrokinetic simulation of ion temperature gradient turbulence. © 2012 American Institute of Physics. [<http://dx.doi.org/10.1063/1.3698309>]

I. INTRODUCTION

Descriptions of turbulent cascades generally focus on the inertial range where scaling and self similarity provide powerful tools for describing the energy transfer between scales.^{1,2} In the dissipation range, where self similarity and scale invariance are broken, cascading to smaller scales continues, albeit with energy losses to dissipation.³ Measurements in laboratory, space, and astrophysical plasmas have begun to probe scales where dissipation arises^{4–8} and much can be learned by comparisons with theoretical models that account for dissipation in the turbulent cascade.

In plasmas, dissipation range cascades have a variety of complications that affect the spectrum and which can be probed and better understood by measurement and comparisons. There are multiple fluctuation fields with potentially different dissipation rates, similar to what occurs in thermal convection at different Prandtl numbers.⁹ There are situations where the spectral transfer rate is modified by inertial effects, such as intermittency or when turbulently interacting vector fields become increasingly aligned at smaller scales.¹⁰ In certain situations there are kinetic effects, which effectively put the turbulence in a phase space with velocity and spatial coordinates.^{11,12} From one situation to the next, the form and nature of dissipation can change radically. In all of these cases, the fundamental interaction between dissipation and turbulent energy transfer is modified. For all, it is

desirable to have a set of general principles with which to describe this interaction.

There are also important issues that arise from the boundedness and inhomogeneity that generally accompany instability. In unbounded plasmas and in laboratory plasmas at sufficiently small scales for boundary conditions to have little effect on the dynamics, dissipation ranges naturally arise at small scales, just as in hydrodynamic turbulence. This is to be expected whenever the dissipation rate grows faster as a function of wavenumber than does the eddy turnover rate or some other appropriate measure of the nonlinear energy transfer rate. However, it has recently been shown that instability-driven plasma turbulence, as is found for example in magnetic fusion devices, has significant energy dissipation in the same scales as the instability drive.¹³ In this situation, the turbulence is born in a dissipation range. Not only is there no inertial range in the scales where the instability is saturated, but also there is no separation between driven scales and dissipated scales. This situation is very unlike the arrangement of driving and dissipation assumed in high Reynolds number hydrodynamic turbulence and is not uncommon in plasmas.¹⁴ It occurs because dispersion relations with instability in one root have other roots that are damped for the scales of the instability, and these are excited nonlinearly by three wave coupling.¹⁵ We wish to know whether the physics of this large scale dissipation range has any connection or similarity to the classical small-scale dissipation range.

In this paper, we describe physical principles that apply to dissipation range turbulent cascades in plasmas for a wide

^{a)}Paper GI3 1, Bull. Am. Phys. Soc. **56**, 94 (2011).

^{b)}Invited speaker.

variety of turbulent situations with different forms of dissipation. These principles can be used to derive spectra and compare with experimental measurements or observations from simulations. After setting out the principles, we illustrate their application in several situations. For each illustration, a dissipation range spectrum is derived. A recent paper derived dissipation range spectra for MHD with magnetic Prandtl number $Pm \leq 1$.¹⁶ Our first illustration takes up the case of MHD with $Pm > 1$ and considers situations with and without scale-dependent alignment of the magnetic and flow fields. We next consider a general case with arbitrary dissipation that scales in wavenumber space. The third illustration is tokamak microturbulence. We develop an approximation for the asymptotic spectrum of ion temperature gradient (ITG) turbulence where there is dissipation from damped modes in the wavenumber range of the instability drive. We then consider comparisons with experiment and simulation and look at three cases. These are magnetic turbulence in liquid metal from measurements in the Madison dynamo experiment (MDE),⁸ magnetic turbulence in a plasma from the Madison symmetric torus (MST),¹⁷ and ITG turbulence from a gyrokinetic model.¹⁸

Because this work explores a new area, the effects considered do not include everything that might be pertinent to observations. Anisotropy, two-fluid, and kinetic effects are not treated in the MHD model. For ITG turbulence, kinetic effects and anisotropy intrinsic to the gyrokinetic model enter empirically in the modeling of the amplitude dependent dissipation from damped modes, but these effects are not treated explicitly. Comparisons are therefore exploratory and preliminary.

II. GENERAL PHYSICAL PRINCIPLES

The self similarity of inertial range energy transfer is predicated on two hypotheses. One is that the nonlinearity has no intrinsic scale. The other is that dissipation is negligible on dynamical (nonlinear) time scales, essentially guaranteeing that no energy is lost to dissipation in the interactions that carry energy from one scale to the next. With these hypotheses, the energy transfer rate T_k at each scale k^{-1} is equal to the energy input rate ϵ . For Navier-Stokes turbulence $T_k = v_k^3 k$, where v_k is the flow, yielding the Kolmogorov result $v_k \propto \epsilon^{1/3} k^{-1/3}$, or $E(k) \propto \epsilon^{2/3} k^{-5/3}$, where $E(k) = v_k^2/k$ is the spectrum.

In reality, dissipation is not zero in the inertial range, but its rate is merely small compared to the energy transfer rate. Its magnitude scales with wavenumber, as does the ratio of energy transfer rate to dissipation rate, $R = T_k / \mu k^2 E(k)$, where μ is the viscosity. Using the expressions above, $R = \epsilon^{1/3} \mu^{-1} k^{-4/3}$, from which we see that $R \gg 1$ for k small, $R = 1$ for some scale $k_d = \epsilon^{1/4} / \mu^{3/4}$, and $R \ll 1$ for k large. (When k is a system scale, R is the Reynolds number; k_d is the Kolmogorov wavenumber, generally taken to be the wavenumber that separates the inertial range from the dissipation range.) The scaling of R indicates that nonlinear transfer coexists with dissipation *at all scales*, and therefore, that dissipation should be scaled into the dynamical balance that yields the energy spectrum, along with ϵ and T_k .

When this is done under a variety of closure schemes [which relate T_k to $E(k)$], the spectrum assumes the form

$$E(k) = a \epsilon^{2/3} k^{-5/3} \exp\left\{-b\left(\frac{k}{k_d}\right)^\alpha\right\}, \quad (1)$$

where a and b are constants, and α is a number whose value falls between 1 and 2, depending on the closure.^{3,19–24} The exponential function in which dissipation resides applies over the entire spectrum. With $\alpha > 0$, it makes an increasingly negligible correction to the power law as k becomes much smaller than k_d . Conversely, the power law also holds over the entire spectrum, but its correction to the exponential is increasingly negligible for k much greater than k_d . For energy to progress to smaller scales beyond k_d , nonlinear energy transfer must remain operative. The continuation of the power law for $k > k_d$ simply asserts that the transfer retains its inertial scaling and self similarity even as dissipation removes a greater fraction of energy remaining in the cascade. We know of no proof that these inertial properties must continue into the dissipation range $k > k_d$, but the hypothesis seems reasonable by Occam's razor.

A simple and physically appealing scaled balance between dissipation and energy transfer is

$$-\mu k^2 E(k) = \frac{dT_k}{dk}, \quad (2)$$

which asserts that dissipation attenuates “propagation” of energy to higher k . Under a simple procedure by Tennekes and Lumley that incorporates the inertial balance $\epsilon = T_k$ into the dissipative balance Eq. (2), the latter can be solved to yield Eq. (1) with $\alpha = 4/3$.³ There is some evidence that $\alpha = 1$ may be physically more realistic. We are interested primarily in an intuitive basis for discussing and assessing dissipation range effects in plasmas. Equation (2) provides a straightforward and transparent means for doing so and will be adopted in this paper as the central construct for describing energy cascades in the presence of dissipation.

The effects we will consider fall in three categories, namely (1) modifications of the wavenumber scaling of the nonlinear transfer strength T_k , (2) modifications of the wavenumber scaling of the dissipation rate, and (3) nonlocal effects (in wavenumber) from multiple fluctuation fields with different dissipation rates.

A. Transfer strength scaling

According to Eq. (1), the nonlinear transfer rate T_k is not constant across the entire spectrum. If some nonlinear process makes T_k stronger as k increases, it is expected from Eq. (2) that attenuation by dissipation becomes less efficient relative to nonlinear transfer and exponential falloff weakens. Conversely, if some process makes T_k weaker as k increases, attenuation becomes more efficient relative to transfer and exponential falloff is steeper. An example of a nonlinear process that changes the strength of T_k as a function of k is intermittency as described by an eddy mitosis model.²⁵ The steeper inertial range spectrum $E(k) = \epsilon^{2/3} k^{-5/3} (kl_0)^{-(3-D)/3}$, where $D < 3$ and l_0 is a system scale, implies that intermittency

makes T_k stronger as k increases and leads to a slower exponential falloff.

In plasma models, there are different forms for the nonlinearities and hence different transfer rates T_k . For MHD, the nonlinear transfer for the flow equation is $T_v(k) = \int \{\mathbf{v} \cdot (\mathbf{v} \cdot \nabla) \mathbf{v} - \mathbf{v} \cdot (\mathbf{B} \cdot \nabla) \mathbf{B}\} \exp[i\mathbf{k} \cdot \mathbf{x}] d^3x$, where \mathbf{v} and \mathbf{B} are the flow and magnetic field. This form is clearly sensitive to the nonlinear orientation of the vectors \mathbf{v} and \mathbf{B} . If \mathbf{v} and \mathbf{B} become increasingly aligned as k increases, it has been shown that T_k becomes weaker. This type of scale dependent dynamic alignment is postulated to occur in MHD turbulence.¹⁰ Referring to Eq. (1), it makes the exponent of k in the power law less negative and increases the value of α . Examples are given in Ref. 16.

B. Dissipation rate scaling

The viscous dissipation of hydrodynamics goes as μk^2 . Resistivity and isotropic viscosity in MHD also scale as k^2 . This is a common scaling for dissipative terms in fluid models, including plasma models. In kinetic theory, the irreversible dissipation is governed by collision operators and may not have the same scaling with wavenumber. Moreover, there is another critical concern regarding dissipation in plasma turbulence driven by instability. Recent work shows that damped modes are excited in instability driven turbulence in the same wavenumber range as the instability.^{11,14} This produces a nonlinear (i.e., amplitude dependent) damping rate that is not given by linear rates such as μk^2 , either in magnitude or in scaling. While spectra can still be formulated, the damping at finite amplitude must be used in place of linear damping rates.

In general, if dissipation is known and represented by a coefficient times k to a power δ , the exponential falloff of the spectrum will be steeper (α larger) if δ is larger, and smaller (α smaller) if δ is smaller. This will be illustrated in Secs. III B and III C.

C. Differential dissipation and nonlocality

When turbulence involves multiple fluctuation fields with different rates of dissipation, each field has a different wavenumber k_d , which for discussion purposes we call k_{d1} and k_{d2} with $k_{d1} < k_{d2}$. This occurs in well known circumstances for thermal convection with Prandtl number $P \neq 1$ and in MHD with magnetic Prandtl number $Pm \neq 1$, where $P = \mu/\chi$ is the ratio of viscosity to thermal conductivity and $Pm = \mu/\eta$ is the ratio of viscosity to resistivity. In these systems, all dissipation rates scale as k^2 , but the same situation arises if there are other scalings. Contrary to a simplistic extension of Eq. (1) to each field, the field with k_{d1} need not be dominated by exponential decay for $k_{d1} < k < k_{d2}$. Instead it is possible for nonlocal wavenumber interactions between fluctuations at $k > k_{d1}$ and $k' < k_{d1}$ to sustain some type of power law falloff. For example, in MHD turbulence with $Pm < 1$, $\eta > \mu$, where η is the resistivity. Thus $k_{d1} \equiv k_\eta < k_\mu \equiv k_{d2}$. In the range $k_\eta < k < k_\mu$, the magnetic energy is not dominated by exponential decay. Through the nonlocal interaction of $B_k, B_{k'}$ and $v_{k-k'}$, where $k' < k_\eta$, the magnetic energy is dominated by a power law with the

exponent 11/3.^{26,27} For $k > k_\mu$, all fields are dominated by exponential decay in a way that can be extracted from balances like that of Eq. (2).¹⁶

In thermal convection for $P > 1$, $k_{d1} \equiv k_\mu < k_\chi \equiv k_{d2}$, where χ is the thermal conductivity. The temperature fluctuation is a passive scalar convected by the turbulent flow. For $k > k_\mu$, the flow is dominated by exponential decay, but the convected temperature is not. Rather, small scale temperature structure for $k > k_\mu$ is nonlocally convected by large scale flow with $k' < k_\mu$, leading to decay for $E_T(k) = T_k^2/k$ dominated by a power law in the same wavenumbers for which the flow is dominated by exponential decay.⁹ This situation is believed to apply to MHD turbulence for $Pm > 1$,²⁸ and is described in Sec. III.

III. ILLUSTRATIONS

To illustrate the dissipation range effects introduced above, we consider three dissipation range situations in plasma physics that were not considered in earlier work.¹⁶ The comparisons, which follow in Sec. IV, will relate both to some new calculations in this section and to earlier calculations.

A. $Pm > 1$ MHD turbulence

1. Unaligned turbulence

MHD turbulence with $Pm \neq 1$ illustrates both the effect of scaled changes in the energy transfer rate and nonlocal interaction regimes when the dissipation rates of two fluctuation fields are unequal. Previous work derived spectra for $Pm \leq 1$,¹⁶ here we consider $Pm > 1$. The resistive incompressible MHD equations are

$$\frac{\partial \mathbf{v}}{\partial t} + \mathbf{v} \cdot \nabla \mathbf{v} - \mathbf{B} \cdot \nabla \mathbf{B} = -\nabla \left[p + \frac{B^2}{2} \right] + \mu \nabla^2 \mathbf{v}, \quad (3)$$

$$\frac{\partial \mathbf{B}}{\partial t} + \mathbf{v} \cdot \nabla \mathbf{B} - \mathbf{B} \cdot \nabla \mathbf{v} = \eta \nabla^2 \mathbf{B}, \quad (4)$$

where all symbols have their usual meanings and the viscosity μ is isotropic. A factor $1/\sqrt{4\pi\rho}$ has been absorbed into the variable \mathbf{B} , where ρ is the mass density. There are two dissipated transfer balances, one for each field, given by

$$-2\mu E_v(k)k^2 = \frac{dT_v}{dk}, \quad (5)$$

$$-2\eta E_B(k)k^2 = \frac{dT_B}{dk}, \quad (6)$$

where $E_v(k)$ and $E_B(k)$ are the spectral power densities associated with flow and magnetic field fluctuation, defined by $E_v(k) = \int v^2 \exp[i\mathbf{k} \cdot \mathbf{x}] d^3x$ and $E_B(k) = \int B^2 \exp[i\mathbf{k} \cdot \mathbf{x}] d^3x$. The spectral energy transfer rates $T_v(k)$ and $T_B(k)$ are

$$T_v(k) = \int \{\mathbf{v} \cdot (\mathbf{v} \cdot \nabla) \mathbf{v} - \mathbf{v} \cdot (\mathbf{B} \cdot \nabla) \mathbf{B}\} \exp[i\mathbf{k} \cdot \mathbf{x}] d^3x, \quad (7)$$

$$T_B(k) = \int \{\mathbf{B} \cdot (\mathbf{v} \cdot \nabla) \mathbf{B} - \mathbf{B} \cdot (\mathbf{B} \cdot \nabla) \mathbf{v}\} \exp[i\mathbf{k} \cdot \mathbf{x}] d^3x. \quad (8)$$

Solution of Eqs. (5) and (6) for $E_v(k)$ and $E_B(k)$ requires that $T_v(k)$ and $T_B(k)$ be expressed in terms of $E_v(k)$ and $E_B(k)$. This step constitutes a closure and is subject to subtleties that lie outside the scope of the present work. Moreover, there are multiple possibilities for forming the closure, with different outcomes, which will require more information from experiments and simulations to validate. We know from simulations that the magnetic energy enters a regime where $E_B \propto k^{-1}$ for $k > k_\mu$,²⁸ and we will ensure that our closure captures this behavior. Our guide is thermal convection for $P > 1$, where temperature fluctuations are essentially a passive scalar field and found to decay as k^{-1} .⁹ With B as a passive scalar by analogy, T_v is closed as in hydrodynamics. Following the procedure of Tennekes and Lumley,³

$$\begin{aligned} T_v &= v_k^3 k = v_k \frac{v_k^2}{k} k^2 = v_k E_v(k) k^2 = \epsilon^{1/3} k^{-1/3} E_v(k) k^2 \\ &= \epsilon^{1/3} E_v(k) k^{5/3}. \end{aligned} \quad (9)$$

In this procedure, the inertial range spectrum is used to write v_k as a function of k . This incorporates the forcing as a boundary condition. In developing Eq. (9), we assume that \mathbf{v} and \mathbf{B} do not have scale-dependent alignment. The effects of alignment will be taken up shortly. Substituting Eq. (9) into Eq. (5) and solving yields

$$E_v(k) = \epsilon^{2/3} k^{-5/3} \exp\left[-\frac{3}{2} \left(\frac{k}{k_{\mu_{un}}}\right)^{4/3}\right], \quad (10)$$

for all k , where $k_{\mu_{un}} = \epsilon^{1/4}/\mu^{3/4}$.

Under the passive scalar argument, T_B is governed by its first term in Eq. (8), $T_B = (\mathbf{v} \cdot \nabla) B^2$. Following Batchelor,

$$(\mathbf{v} \cdot \nabla) B^2 \rightarrow v_{k_{\mu_{un}}} k_{\mu_{un}} B_k^2 = v_{k_{\mu_{un}}} k_{\mu_{un}} E_B(k) k, \quad (11)$$

where the scale k is in the range intermediate to the viscous and resistive Kolmogorov scales $k_{\mu_{un}} < k < k_{\eta_{un}}$. The treatment $\mathbf{v} \cdot \nabla \rightarrow v_{k_{\mu_{un}}} k_{\mu_{un}}$ acknowledges that $k_{\mu_{un}}$ is the smallest inertial scale in the flow, with still smaller scales being exponentially small and negligible. The combination $v_{k_{\mu_{un}}} k_{\mu_{un}}$ is the Lagrangian straining rate. An alternative combination $v_{k_{\mu_{un}}} k$ is not a proper nonlinear decorrelation rate because, as an Eulerian sweeping rate, it does not distort fluctuations at scale k . The triad interaction of Eq. (11) is a nonlocal interaction in wavenumber space. It involves a scale $k' = k_{\mu_{un}}$ in the inertial range and scales k and $k - k' \approx k$ in the viscous dissipation range $k > k_{\mu_{un}}$.

Noting that $v_{k_{\mu_{un}}} k_{\mu_{un}} = (\epsilon/\mu)^{1/2}$, Eq. (6) becomes

$$-2\eta E_B(k) k^2 = \frac{d}{dk} \left[(\epsilon/\mu)^{1/2} E_B(k) k \right]. \quad (12)$$

Its solution is

$$E_B(k) = ck^{-1} \exp\left[-\frac{1}{2} \left(\frac{k}{k_{\eta_{un}}}\right)^2\right] (k \geq k_{\mu_{un}}), \quad (13)$$

where c is a constant and $k_{\eta_{un}} = \epsilon^{1/4}/\eta^{1/2}\mu^{1/4} = k_{\mu_{un}} Pm^{1/2}$. This spectrum is dominated by the k^{-1} power law until $k = k_{\eta_{un}}$, after which the exponential dominates. Note that the passive scalar advection of B , as given in Eq. (11), yields a relatively weak increase of T_B with k . This translates into a shallow k^{-1} power-law falloff and a steep exponential falloff with a power 2 in the argument of the exponent. The reason for this behavior is that the relatively slow eddy turnover rate does not move energy quickly through inertial scales, giving shallow power law decay, while it allows large dissipation in a nonlinear correlation time, giving rapid exponential decay once $k > k_{\eta_{un}}$.

The constant c in Eq. (13) can be calculated from the continuity of E_B at $k = k_{\mu_{un}}$. If we assume that E_B is in equipartition with E_v in the inertial range $k < k_{\mu_{un}}$, the magnetic spectrum in these scales is given by

$$E_B(k) = \epsilon^{2/3} k^{-5/3} \exp\left[-\frac{3}{2} \left(\frac{k}{k_{\mu_{un}}}\right)^{4/3}\right], \quad (k \leq k_{\mu_{un}}). \quad (14)$$

Equating Eqs. (13) and (14) at $k = k_{\mu_{un}}$, c is found to be $c = \epsilon^{2/3} (\epsilon^{1/4}/\mu^{3/4})^{-2/3} \exp[(\eta/2\mu) - 3/2] = (\epsilon\mu)^{1/2} \exp[(2Pm)^{-1} - 3/2]$. With this constant, the magnetic energy spectrum for $k \geq k_{\mu_{un}}$ is

$$\begin{aligned} E_B(k) &= k^{-1} (\epsilon\mu)^{1/2} \exp\left[\frac{1}{2} Pm^{-1} - \frac{3}{2} - \frac{1}{2} \left(\frac{k}{k_{\eta_{un}}}\right)^2\right], \\ &\quad (k \geq k_{\mu_{un}}). \end{aligned} \quad (15)$$

It might be argued that near $k = k_{\mu_{un}}$, nonlinear transfer is not sufficiently fast to maintain equipartition given the stronger dissipation in E_v relative to E_B . Then the magnetic spectrum for $k < k_{\mu_{un}}$ would be $E_B(k) = \epsilon^{2/3} k^{-5/3} \exp[-(3/2)(k/k_{\eta_{un}})^{4/3}]$, where the exponential factor is closer to unity than that of Eq. (14) because $k_{\eta_{un}}$ appears in place of $k_{\mu_{un}}$. The slightly modified magnetic spectrum for $k < k_{\mu_{un}}$ yields a slightly modified constant $c = (\epsilon\mu)^{1/2} \exp[(1/2)Pm^{-1} - (3/2)Pm^{-2/3}]$.

2. Aligned turbulence

In MHD, the magnitudes of the nonlinear transfer rates T_v and T_B are sensitive to whether the vector fields \mathbf{v} and \mathbf{B} are largely perpendicular or more parallel. When the degree of vector alignment is scale dependent, the spectrum acquires a different power law.¹⁰ According to Eqs. (5) and (6), it also acquires a different exponential decay. Alignment has its most elegant expression in terms of Elsässer variables $\mathbf{Z}_+ = \mathbf{v} + \mathbf{B}$ and $\mathbf{Z}_- = \mathbf{v} - \mathbf{B}$. Representing the two variables with the notation \mathbf{Z}_\pm , the MHD equations become

$$\begin{aligned} \frac{\partial \mathbf{Z}_\pm}{\partial t} + \mathbf{Z}_\mp \cdot \nabla \mathbf{Z}_\pm &= -\nabla \left[p + \frac{B^2}{2} \right] + \frac{(\mu + \eta)}{2} \nabla^2 \mathbf{Z}_\pm \\ &\quad + \frac{(\mu - \eta)}{2} \nabla^2 \mathbf{Z}_\mp. \end{aligned} \quad (16)$$

The transfer attenuation balances are

$$-2(\mu + \eta)E_{\pm}k^2 + 2(\mu - \eta)k^2 \int \mathbf{Z}_+ \cdot \mathbf{Z}_- \exp[i\mathbf{k} \cdot \mathbf{x}] d^3x \\ = \frac{dT_{\pm}}{dk}, \quad (17)$$

where $E_{\pm}(k) = \int Z_{\pm}^2 \exp[i\mathbf{k} \cdot \mathbf{x}] d^3x$ and $T_{\pm}(k) = \int \mathbf{Z}_{\pm} \cdot (\mathbf{Z}_{\mp} \cdot \nabla) \mathbf{Z}_{\pm} \exp[i\mathbf{k} \cdot \mathbf{x}] d^3x$. Alignment affects the magnitude of $\mathbf{Z}_{\pm} \cdot (\mathbf{Z}_{\mp} \cdot \nabla) \mathbf{Z}_{\pm}$ and can be expressed as a scaled factor Θ_k in a form of T_{\pm} that uses magnitudes of \mathbf{Z}_{\pm}

$$T_{\pm}(k) = Z_{\pm}^2 Z_{\mp} \Theta_k k. \quad (18)$$

When Θ_k is independent of k , there is no scale dependent alignment and the results of unaligned turbulence are recovered. When Θ_k decreases with k , T_{\pm} becomes weaker with increasing k , producing a spectrum with a shallower power law falloff. Simulations suggest that the spectra of MHD turbulence should decay as $k^{-3/2}$,²⁹ and this decay rate is obtained in an inertial balance $\epsilon = T_{\pm}(k)$ when $\Theta_k = \epsilon^{1/4}/V_A^{3/4}k^{1/4}$.

We assume that $v^2 = B^2$, which gives $\mathbf{Z}_+ \cdot \mathbf{Z}_- = 0$ in Eq. (17). To solve Eq. (17), we substitute $\Theta_k = \epsilon^{1/4}/V_A^{3/4}k^{1/4}$ into Eq. (18) and use the closure $T_{\pm}(k) = \mathbf{Z}_{\mp} E_{\pm}(k) k^2 \Theta_k = E_{\pm}(k) \epsilon^{1/2} k^{3/2} / V_A^{1/2}$, where \mathbf{Z}_{\mp} is taken from the inertial balance $\epsilon = \mathbf{Z}_{\mp}^3 \Theta_k k$. The resulting spectra are

$$E_{\pm}(k) = \epsilon^{1/2} V_A^{1/2} k^{-3/2} \exp \left[-\frac{4}{3} \left(\frac{k}{k_{\mu_{al}}} \right)^{3/2} \right], \quad (19)$$

where $k_{\mu_{al}} = 2^{2/3} \epsilon^{1/3} / V_A^{1/3} (\eta + \mu)^{2/3}$. We note that relative to the comparable spectrum for unaligned turbulence, Eq. (10), the power law falloff is shallower and the exponential falloff is steeper, consistent with the scale dependent reduction of T_{\pm} caused by alignment.

Equation (19) represents the spectra of aligned turbulence in the inertial range $k < k_{\mu_{al}}$. In the dissipation range, alignment ceases to depend on scale. This is observed in simulations³⁰ for $Pm = 1$. It is not unexpected for $Pm > 1$, given the very different nonlinear processes in E_v and E_B represented by the nonlocal straining of a passive B . To derive the spectra for $k > k_{\mu_{al}}$, we first convert E_{\pm} to E_v and E_B . For $\mathbf{v} \cdot \mathbf{B}$ small, $E_{\pm}(k) = v_k^2 + B_k^2 \pm 2\mathbf{v} \cdot \mathbf{B} \approx v_k^2 + B_k^2$, and $E_v(k) = E_B(k) = a_{<} k^{-3/2} \epsilon^{1/2} V_A^{1/2} \exp[-4/3(k/k_{\mu_{al}})^{3/2}]$ for $k \leq k_{\mu_{al}}$, where $a_{<}$ is a constant. For $k > k_{\mu_{al}}$, where there is no scale dependent alignment, we have $E_v(k) = a_{>} \epsilon^{2/3} k^{-5/3} \exp[-(3/2)(k/k_{\mu_{un}})^{4/3}]$, where $a_{>}$ is a constant and $k_{\mu_{un}} = \epsilon^{1/4} / \mu^{3/4}$ as before. We choose $a_{>}$ to match these spectra at $k = k_{\mu_{al}}$, yielding

$$a_{>} = a_{<} \epsilon^{-1/6} k_{\mu_{al}}^{1/6} V_A^{1/2} \exp \left[-\frac{4}{3} + \frac{3}{2} \left(\frac{k_{\mu_{al}}}{k_{\mu_{un}}} \right)^{4/3} \right]. \quad (20)$$

The magnetic spectrum for $k > k_{\mu_{al}}$ is $E_B(k) = \hat{c} k^{-1} \exp[-(1/2)(k/k_{\mu_{un}})^2]$, where \hat{c} is a constant and $k_{\mu_{un}} = \epsilon^{1/4} / \mu^{1/4} \eta^{1/2}$, also as before. Again, \hat{c} is chosen by matching at $k_{\mu_{al}}$, yielding

$$\hat{c} = a_{<} \epsilon^{1/2} k_{\mu_{al}}^{-1/2} V_A^{1/2} \exp \left[-\frac{4}{3} + \frac{1}{2} \left(\frac{k_{\mu_{al}}}{k_{\mu_{un}}} \right)^2 \right]. \quad (21)$$

The complete spectra for aligned turbulence in the $Pm < 1$ regime are

$$E_v(k) = E_B(k) = a_{<} k^{-3/2} \epsilon^{1/2} V_A^{1/2} \exp \left[-\frac{4}{3} \left(\frac{k}{k_{\mu_{al}}} \right)^{3/2} \right], \quad (22)$$

$$E_v(k) = a_{<} k^{-5/3} \epsilon^{1/2} V_A^{1/2} k_{\mu_{al}}^{1/6} \exp \left[-\frac{4}{3} + \frac{3}{2} \left(\frac{k_{\mu_{al}}}{k_{\mu_{un}}} \right)^{4/3} - \frac{3}{2} \left(\frac{k}{k_{\mu_{un}}} \right)^{4/3} \right], \quad (k \geq k_{\mu_{al}}), \quad (23)$$

$$E_B(k) = a_{<} k^{-1} \epsilon^{1/2} V_A^{1/2} k_{\mu_{al}}^{-1/2} \exp \times \left[-\frac{4}{3} + \frac{1}{2} \left(\frac{k_{\mu_{al}}}{k_{\mu_{un}}} \right)^2 - \frac{1}{2} \left(\frac{k}{k_{\mu_{un}}} \right)^2 \right], \quad (k \geq k_{\mu_{al}}). \quad (24)$$

Aside from the constants that ensure continuity across $k = k_{\mu_{al}}$, the dissipation range spectra for aligned turbulence are the same as those for unaligned turbulence. The only difference is the inertial part of the spectrum with its shallower power law and steeper exponential.

B. Turbulence with general scaled damping

Consider the scaled attenuation of spectral energy transfer by a generalized damping rate $\gamma_0(k/k_0)^{\delta}$, where γ_0 and δ are constants. Our object is to determine how the exponent α of Eq. (1) depends on δ , i.e., how the rate of exponential decay relates to the rate of dissipation. The spectrum balance is given by

$$-\gamma_0 \left(\frac{k}{k_0} \right)^{\delta} E(k) = \frac{dT_k}{dk}, \quad (25)$$

where for simplicity we will consider advective turbulence with $T_k = v_k^3 k$. Following Ref. 3, T_k is assumed to be proportional to $E(k)$, yielding $T_k = (v_k^2/k) v_k k^2 = E(k) v_k k^2$. For the flow v_k , we substitute from the solution of $\epsilon = T_k$, or $v_k = \epsilon^{1/3} k^{-1/3}$, yielding $T_k = E(k) \epsilon^{1/3} k^{5/3}$. Substituting this into Eq. (25),

$$-\gamma_0 \left(\frac{k}{k_0} \right)^{\delta} E(k) = \epsilon^{1/3} k^{2/3} \left[\frac{5}{3} E(k) + k \frac{dE(k)}{dk} \right]. \quad (26)$$

The solution is

$$E(k) = \begin{cases} a \epsilon^{2/3} k^{-5/3} \exp \left[-\frac{\gamma_0 \epsilon^{-1/3} k^{(\delta-2/3)}}{(\delta-2/3) k_0^{\delta}} \right] & \text{for } \delta \neq 2/3 \\ a \epsilon^{2/3} k^{-5/3} k^{-[\gamma_0 \epsilon^{-1/3} / k_0^{\delta}]} & \text{for } \delta = 2/3. \end{cases} \quad (27)$$

For $\delta \neq 2/3$, Eq. (27) can be put in the form of Eq. (1) with $\alpha = \delta - 2/3$, $b = (\delta - 2/3)^{-1}$, and

$$k_d = \left(\frac{e^{1/3} k_0^\alpha}{\gamma_0} \right)^{\frac{1}{\delta-2/3}}. \quad (28)$$

We observe that for $\delta = 2$ and $\gamma_0 = \mu$ ($k_0 = 1$), Eq. (27) recovers the hydrodynamic dissipation range spectrum for the closure of Ref. 3, including the appropriate Kolmogorov wavenumber. For $\delta > 2/3$, larger values of δ produce a steeper exponential decay and smaller values produce a shallower decay. $\delta = 2/3$ is a special case in which the nonlinear transfer rate and dissipation rate have the same variation with k , keeping the ratio of these two rates equal over the entire spectrum. There is no division between inertial and dissipation ranges and the spectrum is a power law for all k , albeit with a modified spectral index. In this spectrum, despite the power law form, there is dissipation at all wavenumbers. For $\delta < 2/3$, the exponent of k in the argument of the exponential function becomes negative and the overall sign of the argument becomes positive. This causes the exponential to become increasingly weak for $k > k_d$, yielding a spectrum that is asymptotically a power law as $k \rightarrow \infty$. For $k < k_d$, the argument of the exponential is greater than unity and the effect of dissipation is significant. For this type of dissipation scaling, the inertial and dissipation ranges exchange places across k_d relative to their arrangement in hydrodynamics. This unusual arrangement simply follows from having a dissipation rate which becomes weaker than the nonlinear transfer rate at high k . Turbulence with a damping rate corresponding to $\delta < 2/3$ is not a hypothetical situation. In Secs. III C and IV C, we show that gyrokinetic models of ITG turbulence have a nonlinear damping rate with $\delta < 2/3$, and a spectrum that becomes a power law asymptotically for k large.

C. Ion temperature gradient turbulence

Plasma turbulence in magnetic fusion devices is driven by instabilities. The instability that dominates the turbulence drive is a root of a dispersion relation with many additional roots, generally. Most of the additional roots are damped. When the modes corresponding to these damped roots are excited by nonlinear mode coupling, there is an energy sink whose rate is nonlinear and not given by linear damping terms such as viscosity μk^2 or resistivity ηk^2 . Moreover, because damped modes are excited in the same wavenumber range as the instability, the damping rate need not increase strongly with k .

The damping rate associated with nonlinearly excited damped modes is a function of the saturated state and must be determined from it. This has been done numerically for ITG turbulence using the comprehensive toroidal gyrokinetic code GENE (Ref. 18) for the CYCLONE base case.³¹ The damped modes that are excited to finite amplitude number in the thousands. The damping rate in saturation is calculated from the conserved (in absence of drive and dissipation) energylke quantity $U_k = \int dv_{||} d\mu dz B_0 \pi n_0 T_0 |g|^2 / F_0 + \int dz D(k_{\perp}, z) |\phi|^2$, where g is the gyrokinetic distribution, ϕ is the electrostatic

potential, B_0 , n_0 , and T_0 are the equilibrium magnetic field, background density, and background temperature, and D is a function of perpendicular wavenumbers and distance z along the field. The five gyrokinetic coordinates are here represented by z , magnetic moment μ , parallel velocity $v_{||}$, and, upon Fourier transform, the two perpendicular wavenumbers. This energy is conservatively transferred by the nonlinearity, generated by the instability drive, and damped by dissipative processes. The drive and damping can be calculated by taking $\partial U / \partial t$. Part of the construct involves $\partial g / \partial t$. Only dissipative contributions to $\partial g / \partial t$ are retained (linear parts), and other conservative contributions cancel. The result is that $\partial U / \partial t$ is restricted to drive and damping, and excludes the conservative nonlinear transfer. When these operations are performed,

$$\left. \frac{\partial U_k}{\partial t} \right|_{N.C.} = Q_k + C_k, \quad (29)$$

where $N.C.$ signifies the nonconservative part of $\partial U / \partial t$, $Q_k = \int dv_{||} d\mu dz \pi (n_0 T_0 B_0 / L_T) (v_{||}^2 + \mu B_0) g^* i k_y \bar{\phi}$ is proportional to the heat flux, C_k represents collisional dissipation and, in simulations, artificial dissipation, L_T is the temperature gradient scale length, and $\bar{\phi}$ is the gyroaveraged potential. The term Q_k includes the linear drive, which makes a positive contribution. Damped modes also contribute to Q_k , making in some cases a positive contribution and in some cases a negative contribution. Damped modes dominate C_k , making a negative contribution. Details can be found in Refs. 11 and 13.

The quantities Q_k and $\gamma = U_k^{-1} C_k$ are plotted in Figs. 1 and 2. The heat flux term Q_k (Fig. 1) is positive, strongly peaked, and localized inside $k = 1.0$. With Q_k very small for $k > 1$, $\partial U_k / \partial t|_{N.C.}$ is governed by C_k in this range. This makes $\gamma = U_k^{-1} C_k$ the damping rate for the system above $k = 1.0$, comparable to the quantity $-\gamma_0 (k/k_0)^{\delta}$ used in Eq. (25). We observe from Fig. 2 that the damping rate increases with k , first quite rapidly and then so gradually that it appears to flatten out above $k = 4.6$. There is not a single power law that fits this variation. For $0.5 < k < 2.0$, the variation of γ is fit by $-\gamma_0 (k/k_0)^{\delta}$ with $\delta = 0.62$. For $2.0 < k < 4.6$, the variation is fit with $\delta = 0.166$ (from the points $k_y = 2.0$ and $k_y = 4.0$). Most of the damping associated with saturation of the instability occurs for $k \leq 2$ where

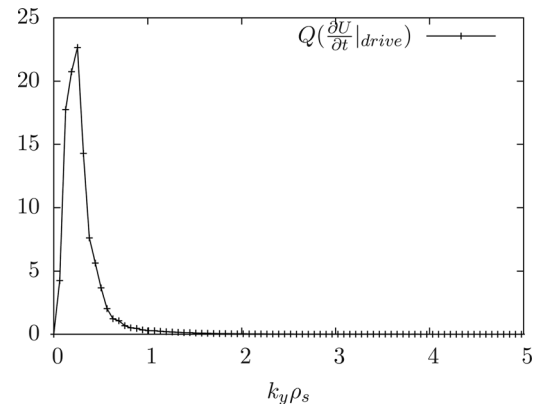


FIG. 1. Variation of the instability drive Q_k as a function of k_y . Q_k peaks inside $k = 0.5$ and is close to zero for $k > 1$.

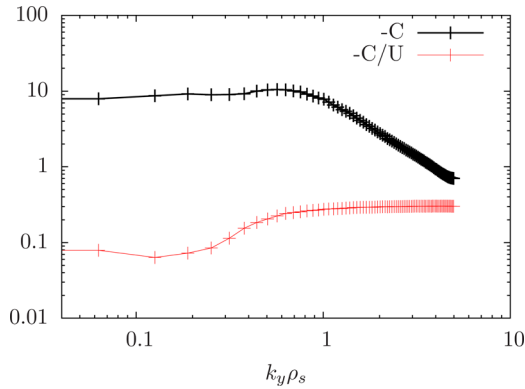


FIG. 2. Variation of the collisional dissipation rate $-C$ and the damping rate $-C_k U_k^{-1}$ as a function of k_y . The damping rate is seen to increase in magnitude above $k \approx 0.2$ with a variation that is quite strong at first and then becomes very gradual.

the instability drive and most fluctuation energy are localized. As an exercise, let us use the power law fit to the variation of γ over the admittedly limited range $2.0 < k < 4.6$. The purpose is to apply the results to Eq. (27) to see what kind of a dissipation range spectrum would occur if the same power law variation in $2.0 < k < 4.6$ continued asymptotically to very large k . Taking $\delta - 2/3 = 0.166 - 2/3$ in Eq. (27) to be -0.5 , the dissipation range spectrum is

$$E_v(k) = a\epsilon^{2/3}k^{-5/3}\exp\left\{\frac{1}{2}\left(\frac{k_d}{k}\right)^{1/2}\right\}, \quad (30)$$

where $k_d = \gamma_0^2/\epsilon^{2/3}$. Because δ actually approaches zero for $k_y > 4.6$, the power $1/2$ in the exponential factor transitions to something closer to $2/3$ for $k_y > 4.6$. Since $k > k_d$, this makes the exponential factor even closer to unity. This spectrum assumes that the nonlinearity $\mathbf{v} \cdot \nabla \mathbf{v}$ governs the nonlinear energy transfer for the power density spectrum $E_v(k) = v_k^2/k = k\phi_k^2$ of $\mathbf{E} \times \mathbf{B}$ flow in gyrokinetics. This assumption may be an oversimplification for gyrokinetics, where other types of cascades and spectra are known to arise.^{12,32} It nevertheless illustrates features that are essential in microinstability driven turbulence and should remain so even in more sophisticated treatments. These are that dissipation is present over all wavenumbers, and that, while it increases gradually with wavenumber, a power law is nonetheless the dominant form of falloff asymptotically for large wavenumber. This is because dissipation is concentrated at low wavenumber in the form of damped modes and increases more slowly for high wavenumber than the nonlinear transfer rate. The result is that the dissipative exponential factor approaches unity from above as $k \rightarrow \infty$ and the spectrum as a whole approaches a power law.

IV. COMPARISONS

The dissipation range physics and spectra discussed above may represent oversimplification of the dynamics in laboratory devices or even simulations with dissipative turbulent transfer. Comparisons, however, are instructive, both to assess the applicability of theory at its present stage of development and to form hypotheses regarding effects that

may be missing or in need of better modeling. It is in this spirit that comparisons with experiment and simulation are undertaken.

A. Madison symmetric torus

Observations of an exponentially decaying magnetic spectrum at small scale (high frequency) in the MST device⁷ provided the original motivation for developing theories of dissipation range turbulence in plasmas. Large scale fluctuations in MST are known to be well modeled by MHD as unstable tearing modes and to launch a cascade to higher wavenumber. While effects of the cascade have been calculated from a model that treats the turbulence as nonlinear Alfvén waves in an infinite homogeneous medium, the role of inhomogeneity (e.g., magnetic shear), two fluid effects, and kinetic effects on the cascade are open questions. The exponentially decaying spectrum applies to the cascade at small scale. It is part of an anisotropy with respect to magnetic field. The magnetic spectrum for perpendicular wavenumber in the electron diamagnetic direction has a clear exponential decay, while the perpendicular wavenumber spectrum in the ion diamagnetic direction has power law decay with a steep k_\perp^{-4} falloff. The power in the electron diamagnetic direction is significantly larger than that of the ion direction, hence the exponential spectrum dominates. The origin of this anisotropy is not understood.

Because the spectrum is exponential, we simply fit a spectrum of the form of Eq. (1) and see how closely it follows the observed spectrum. A fitting exercise for the form $E_B(k_\perp) = k_\perp^{-\beta}\exp[-b(k_\perp/k_\eta)^\alpha]$ returns values $\beta = 1.79$ with 95% confidence bounds of (1.56, 2.02) and $\alpha = 1.64$ with 95% confidence bounds of (1.12, 2.16). To visualize the fit, we choose theoretical values $\beta = -5/3$ and $\alpha = 4/3$ that lie within the confidence bounds. The fit with $E_B(k_\perp) = \epsilon^{2/3}k_\perp^{-5/3}\exp[-3/2(k_\perp/k_\eta)^{4/3}]$ is shown in Fig. 3. The fit is sufficiently good that the results could be easily misconstrued. With two free parameters (ϵ and k_η), there is considerable leeway for optimization. The real test is to see if the returned values for ϵ and k_η are physically reasonable. The returned value for ϵ primarily gauges the measured spectral

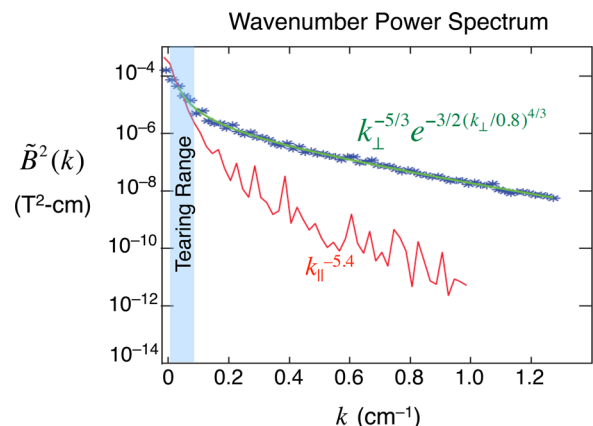


FIG. 3. Perpendicular and parallel wavenumber spectra for magnetic turbulence in MST. The perpendicular wavenumber spectrum is fit to a theoretical spectrum, where the latter is a solid line, and the observed spectrum is indicated by stars.

power and is not particularly telling. The returned value of k_η , however, can be compared to the theoretical value $k_\eta = (\epsilon/\eta^3)^{1/4}$, calculated using the returned value of ϵ and the resistivity computed from local parameters. The fitting gives $k_\eta \approx 0.8 \text{ cm}^{-1}$, while the value from plasma parameters is nearly 4 times larger at $k_\eta = 3 \text{ cm}^{-1}$.

There might be a temptation to dismiss the above exercise as flawed for its failure to account for Pm , or to include anisotropic viscosity, inhomogeneity, kinetic effects, etc. However, independent of any fitting, the spectrum does show exponential falloff, and the simplest conclusion to be drawn from the comparison is that there appears to be a form of dissipation in the spectrum that is stronger than resistivity. An obvious and physically sensible candidate is cyclotron resonant absorption, which is expected to occur in this part of the spectrum, and is already a candidate for observed non thermal ion heating in MST.³³ The comparison thus gives evidence for kinetic dissipation, a process that is suspected in other types of magnetic turbulent cascades. Clearly, improved modeling of the MST spectrum requires the inclusion of ion cyclotron resonant damping, a process that may explain the spectrum anisotropy with respect to the k_\perp direction through the resonance condition.

The fitting exercise also provides support for the central hypothesis that dissipation range cascades combine the self similar transfer of the inertial range with dissipation of energy. Fitting forms that have only exponential decay and do not include the power law behavior do not describe the spectrum shape as well as those that include the power law.

B. Madison dynamo experiment

The MDE is a liquid sodium experiment whose turbulent medium is not a plasma but a liquid metal. MHD is the only applicable model, allowing tests of an important model for plasmas without the complications of plasma processes such as kinetic effects. Liquid sodium has a low magnetic Prandtl number [$O(10^{-5})$] and provides an opportunity for studying the physics of differential dissipation and nonlocality in dissipation range cascades. Magnetic turbulence in this regime has been previously studied in a number of devices.^{34–36}

Spectra for MHD dissipation range turbulence with $Pm < 1$ have been worked out previously.¹⁶ Like the $Pm > 1$ spectra derived above, nonlocal interactions in the wavenumber range intermediate to the two Kolmogorov wavenumbers ($k_\eta < k < k_\mu$) give a dominant power law decay for the more heavily damped field, which in this regime is B , instead of exponential decay. The magnetic spectrum for the unaligned case is

$$E_B(k) = \epsilon^{2/3} k^{-5/3} \exp\left[-\frac{3}{2}\left(\frac{k}{k_{\eta_{un}}}\right)^{4/3}\right] \quad (k \leq k_{\eta_{un}}), \quad (31)$$

$$E_B(k) = \epsilon^{2/3} k^{-11/3} k_{\eta_{un}}^2 \exp\left[-\frac{3}{2}(1 - Pm)\right] \exp\left[-\frac{3}{2}\left(\frac{k}{k_{\mu_{un}}}\right)^{4/3}\right] \quad (k \geq k_{\eta_{un}}), \quad (32)$$

where the Kolmogorov wavenumbers for $Pm < 1$ are $k_{\eta_{un}} = \epsilon^{1/4}/\eta^{3/4}$ and $k_{\mu_{un}} = \epsilon^{1/4}/\mu^{3/4}$. The kinetic energy spectrum goes as $E_v(k) \approx \epsilon^{2/3} k^{-5/3}$ for $k \sim k_{\eta_{un}}$. With $Pm = 10^{-5}$, $k_{\mu_{un}}/k_{\eta_{un}} = (\eta/\mu)^{3/4}$ is nearly 10^4 . The dynamic range of probes used to detect fluctuations of the flow and magnetic field in MDE is not sufficient to access scales from $k_{\eta_{un}}$ to $k_{\mu_{un}}$ and permit observation of exponential decay for $k > k_{\mu_{un}}$. The probes do, however, yield simultaneous measurement of the magnetic and kinetic energy spectra over scales around $k_{\eta_{un}}$. They can check whether there are power-law spectral indices of $-11/3$ and $-5/3$ for magnetic and kinetic energies. The flow is excited by two oppositely facing coaxial impellers. The Reynolds number is large [$O(10^7)$] and the mean flow has large shear, driving highly turbulent flow. A magnetic field imposed by external coils is advected by the flow and becomes turbulent. The regime is kinematic, i.e., $E_v \gg E_B$. While the theory assumes $E_v = E_B$ for $k < k_{\eta_{un}}$, the spectral transfer rates for $k > k_{\eta_{un}}$ are $T_v(k) = \int [\mathbf{v} \cdot (\mathbf{v} \cdot \nabla) \mathbf{v}] \exp[i\mathbf{k} \cdot \mathbf{x}] d^3x$ and $T_B(k) = \int [\mathbf{B} \cdot (\mathbf{v} \cdot \nabla) \mathbf{B} - \mathbf{B} \cdot (\mathbf{B} \cdot \nabla) \mathbf{v}] \exp[i\mathbf{k} \cdot \mathbf{x}] d^3x$ in both cases, yielding identical spectral indices. The only difference between the two cases is an overall offset of E_B from E_v in the kinematic regime. Previous studies on MDE using Hall probes⁸ established that the magnetic energy spectrum undergoes a transition from a spectral index of $-5/3$ to $-11/3$. They also demonstrated the validity of the Taylor hypothesis and showed that the transition wavenumber has a magnitude and scaling consistent with the Kolmogorov wavenumber. Previously there was no diagnostic for the self-consistent simultaneous flow. Laser Doppler velocimetry measurements in a similar experiment in water were used to infer the properties of the flow (non self consistently, of course). The present studies address this limitation, employing a newly developed combined probe that allows simultaneous measurement of the three components of both velocity and magnetic field fluctuations.

The results of measurements using the new probe are displayed in Fig. 4. In the magnetic field, there is a driving range below 4 Hz. Inertial behavior in the flow emerges at

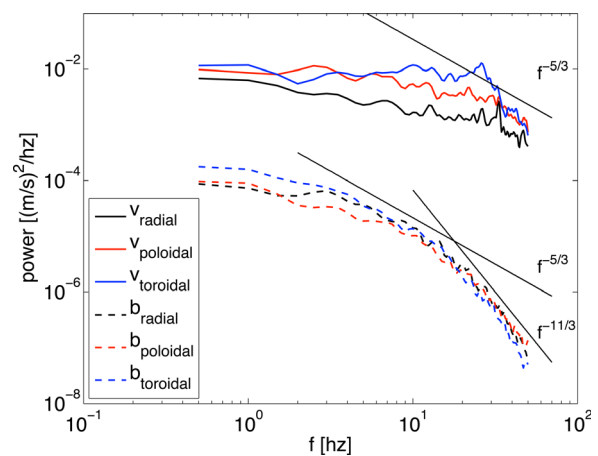


FIG. 4. Kinetic and magnetic energy frequency spectra from the Madison dynamo experiment. The Taylor hypothesis applies to these measurements, so that frequency spectra are indicative of wavenumber spectra. Power law slopes are provided for comparison.

somewhat higher frequencies. Most importantly, the magnetic field shows a transition from a falloff that is consistent with $f^{-5/3}$ to one that is consistent with $f^{-11/3}$ while the flow has a falloff consistent with $f^{-5/3}$ everywhere above the transition from the driving range. As shown previously,⁸ the Taylor frozen-in hypothesis holds in MDE, hence frequency measurements indicate the behavior of the wavenumber spectrum.

C. Gyrokinetic simulation of ITG spectrum

Gyrokinetic simulations of ITG turbulence (CYCLONE Base Case) are well known to be insensitive to resolution in perpendicular wavenumber space, provided the scales for which the linear growth rate is positive are resolved. When higher wavenumbers are included, neither the fluctuation level nor transport rates are significantly changed. This is because damping in and nearby the wavenumber range of the instability from damped modes saturates the instability and fixes turbulence and transport levels. Whatever energy is not dissipated at low wavenumber finds its way to high perpendicular wavenumber where it undergoes a cascade.³⁸ The associated spectrum has been measured in a set of carefully constructed high resolution runs.

Spectra from these simulations are shown in Fig. 3 of Ref. 37. The traces correspond to simulations of trapped electron mode turbulence, electron temperature gradient turbulence, and ion temperature gradient turbulence. All follow power laws asymptotically. Because the amplitude-dependent damping rate has only been calculated for the ITG case (Sec. III C), we focus on that case. The spectrum is for density fluctuations, hence a comparison with the dissipation range theory of Sec. III must determine the relation between the kinetic energy and density spectra. For ITG turbulence, the ions are adiabatic with $n = \phi$. Then $E_v(k) = v^2/k = k^2\phi^2/k = k\phi^2 = kn^2$. The density spectrum is $E_n(k) = n^2/k = E_v(k)/k^2$. From Eq. (30), we find that

$$E_n(k) = a\epsilon^{2/3}k^{-11/3}\exp\left\{\frac{1}{2}\left(\frac{k_d}{k}\right)^{1/2}\right\}, \quad (33)$$

where $k_d = \gamma_0^2/\epsilon^{2/3}$, as before.

The power law part of the spectrum, which dominates the exponential asymptotically for k large, is in agreement with the slope of the simulated spectrum, except for the largest values of k where a non power law feature appears. The latter may be due to small scale electron temperature gradient instability, whose dynamics are included in the model. The dissipation range $k < k_d$ falls in the region of drive, which is not accounted for in Eq. (33). The key conclusion from this comparison is that the dissipation range theory allows for a power law spectrum asymptotically when dissipation is concentrated in large scales and grows with k more slowly than the nonlinear decorrelation rate. Because the energy in the cascade to high k becomes weakly damped as k increases beyond the range displayed in Fig. 2, the spectrum could become nonstationary at very large wavenumbers, or a stronger form of damping might arise at the highest wavenumbers to absorb the energy in the cascade.

V. CONCLUSIONS

Dissipation range cascades in hydrodynamics associated with viscous damping are known to produce an exponential falloff in the wavenumber spectrum. The same type of spectrum is shown here to occur for plasma turbulence. When the scaling properties of the nonlinearity and dissipation apply over all scales, the spectrum is a product of a power law and an exponential factor, both of which apply to all scales. This is the normal situation away from the scales of instability and is shown here to be relevant to several types of plasma turbulence.

A simple procedure developed in hydrodynamics for deriving dissipation range spectra is found to be useful for plasma turbulence. It shows that plasmas introduce effects that modify both the power law and the exponent. These include modifications of the wavenumber scaling of the nonlinear transfer strength, modifications of the wavenumber scaling of the dissipation rate, and nonlocal interactions in wavenumber for situations with multiple fluctuation fields and different dissipation rates. Generally, when the transfer rate becomes weaker with smaller scale, the power law falloff is shallower and exponential decay is stronger. This arises because weaker transfer has a longer nonlinear timescale, which allows greater dissipation in a nonlinear time. This situation occurs when there is scale dependent alignment of vector fields in MHD. It also occurs for $P_m > 1$ MHD turbulence. In this situation, a nonlocal interaction associated with Lagrangian straining of the magnetic field on scales above the viscous Kolmogorov scale by flow on the viscous Kolmogorov scale imparts a shallow k^{-1} falloff to the magnetic energy. When magnetic energy reaches the resistive Kolmogorov scale its exponential fall-off is very strong. Analysis also shows that when damping increases more slowly with wavenumber than the nonlinear transfer rate, dissipation and inertial ranges can trade positions in wavenumber space, with the dissipation range at low k and the inertial range at high k . This occurs for ion temperature gradient turbulence modeled by gyrokinetics, where there is large damping at low k from damped modes.

The above ideas have been tested with three comparisons involving magnetic turbulence in the MST device, low P_m MHD turbulence in the Madison Dynamo Experiment, and gyrokinetic ITG turbulence. They show the relevance of the dissipation cascade analysis described in this paper. The comparison with the exponential spectrum from magnetic turbulence in MST also shows that kinetic effects not present in MHD appear to contribute to the dissipation of turbulent energy.

ACKNOWLEDGMENTS

This work was supported by the National Science Foundation and the U.S. Department of Energy grants. Useful discussions with Fabian Waleffe and Stas Boldyrev are acknowledged.

¹A. N. Kolmogorov, Dokl. Akad. Nauk. SSSR **30**, 9 (1941).

²U. Frisch, *Turbulence* (Cambridge University Press, Cambridge, 1995).

- ³H. Tennekes and J. L. Lumley, *A First Course in Turbulence* (MIT, Cambridge, 1972).
- ⁴R. J. Leamon, C. W. Smith, N. F. Ness, W. H. Matthaeus, and H. K. Wong, *J. Geophys. Res.* **103**, 4775, (1998).
- ⁵C. W. Smith, K. Hamilton, B. J. Vasquez, and R. J. Leamon, *Astrophys. J. Lett.* **645**, L85 (2006).
- ⁶C. C. Chaston, C. Salem, J. W. Bonnell, C. W. Carlson, R. E. Ergun, R. J. Strangeway, and J. P. McFadden, *Phys. Rev. Lett.* **100**, 175003 (2008).
- ⁷Y. Ren, A. F. Almagri, G. Fiksel, S. C. Prager, J. S. Sarff, and P. W. Terry, *Phys. Rev. Lett.* **107**, 195002 (2011).
- ⁸M. D. Nornberg, E. J. Spence, R. D. Kendrick, C. M. Jacobson, and C. B. Forest, *Phys. Plasmas* **13**, 055901 (2006).
- ⁹G. K. Batchelor, *J. Fluid Mech.* **5**, 113 (1959).
- ¹⁰S. Boldyrev, *Astrophys. J. Lett.* **626**, L37 (2005).
- ¹¹D. R. Hatch, P. W. Terry, F. Jenko, and F. Merz, and W. M. Nevins, *Phys. Rev. Lett.* **106**, 115003 (2011).
- ¹²T. Tatsuno, W. Dorland, A. A. Schekochihin, G. G. Plunk, M. Barnes, S. C. Cowley, and G. G. Howes, *Phys. Rev. Lett.* **103**, 015003 (2009).
- ¹³D. R. Hatch, P. W. Terry, F. Jenko, F. Merz, M. J. Pueschel, W. M. Nevins, and E. Wang, *Phys. Plasmas* **18**, 055706 (2011).
- ¹⁴K. Makwana, P. W. Terry, J.-H. Kim, and D. R. Hatch, *Phys. Plasmas* **18**, 012302 (2011).
- ¹⁵P. W. Terry, D. A. Baver, and S. Gupta, *Phys. Plasmas* **13**, 022307 (2006).
- ¹⁶P. W. Terry and V. Tangri, *Phys. Plasmas* **16**, 082305 (2009).
- ¹⁷S. C. Prager, A. F. Almagri, S. Assadi, J. A. Beckstead, R. N. Dexter, D. J. Den Hartog, G. Chartas, S. Hokin, T. W. Lovell, T. D. Rempel, J. S. Sarff, W. Shen, C. W. Spragins, and J. C. Sprott, *Phys. Fluids B* **2**, 1367 (1990).
- ¹⁸F. Jenko, W. Dorland, M. Kotschenreuther, and B. N. Rogers, *Phys. Plasmas* **7**, 1904 (2000).
- ¹⁹A. A. Townsend, *Proc. R. Soc. London, Ser. A* **208**, 534 (1951).
- ²⁰S. Corrsin, *Phys. Fluids* **7**, 1156 (1964).
- ²¹Y. H. Pao, *Phys. Fluids* **8**, 1063 (1965).
- ²²R. H. Kraichnan, *J. Fluid Mech.* **5**, 497 (1959).
- ²³C. Foias, O. Manley, and L. Sirovich, *Phys. Fluids A* **2**, 464 (1990).
- ²⁴A. S. Monin and A. M. Yaglom, *Statistical Fluid Mechanics* (MIT Press, Cambridge, MA, 1975) Vol. II.
- ²⁵U. Frisch, P. L. Sulem, and M. Nelkin, *J. Fluid Mech.* **87**, 719 (1978).
- ²⁶G. S. Golitsyn, Sov. Phys. Dokl. **5**, 536 (1960).
- ²⁷K. Moffatt, *J. Fluid Mech.* **11**, 625 (1961).
- ²⁸D. Biskamp, *Nonlinear Magnetohydrodynamics* (Cambridge University Press, Cambridge, 1993).
- ²⁹W.-C. Müller and R. Grappin, *Phys. Rev. Lett.* **95**, 114502 (2005).
- ³⁰J. Mason, F. Cattaneo, and S. Boldyrev, *Phys. Rev. E* **77**, 036403 (2008).
- ³¹A. M. Dimits, G. Bateman, M. A. Beer, B. I. Cohen, W. Dorland, G. W. Hammett, C. Kim, J. E. Kinsey, M. Kotschenreuther, A. H. Kritz, L. L. Lao, J. Mandrekas, W. M. Nevins, S. E. Parker, A. J. Redd, D. E. Schumaker, R. Sydora, and J. Weiland, *Phys. Plasmas* **7**, 969 (2000).
- ³²M. Barnes, F. I. Parra, and A. A. Schekochihin, *Phys. Rev. Lett.* **107**, 115003 (2011).
- ³³V. Tangri, P. W. Terry, and G. Fiksel, *Phys. Plasmas* **15**, 112501 (2008).
- ³⁴P. Odier, J.-F. Pinton, and S. Faure, *Phys. Rev. E* **58**, 7397 (1998).
- ³⁵A. Alemany, P. Marty, F. Plumian, and J. Soto, *J. Fluid Mech.* **403**, 263 (2000).
- ³⁶A. Gailitis, O. Lielausis, E. Platacis, G. Gerbeth, and F. Stefani, *Phys. Plasmas* **11**, 2838 (2004).
- ³⁷T. Görler and F. Jenko, *Phys. Plasmas* **15**, 102508 (2008).
- ³⁸A. Bañón Navarro, P. Morel, M. Albrecht-Marc, D. Carati, F. Merz, T. Görler, and F. Jenko, *Phys. Rev. Lett.* **106**, 255001 (2011).